



1 **Molecular composition of organic aerosols in central Amazonia: an ultra-high**
2 **resolution mass spectrometry study**

3 I. Kourtchev^{1*}, R.H.M. Godoi², S. Connors¹, J.G. Levine³, A. Archibald^{1,4}, A.F.L. Godoi², S.L.
4 Paralovo², C.G.G. Barbosa², R.A.F. Souza⁵, A.O. Manzi⁶, R. Seco⁷, S. Sjostedt⁸, J.-H. Park⁹,
5 A. Guenther^{7,10}, S. Kim⁷, J. Smith^{11,12}, S.T. Martin^{13,14} and M. Kalberer^{1*}

6 ¹Department of Chemistry, University of Cambridge, Cambridge, CB2 1EW, UK

7 ²Environmental Engineering Department, Federal University of Parana, Curitiba, Brazil

8 ³School of Geography Earth & Environmental Sciences, University of Birmingham,
9 Birmingham, B15 2TT, UK

10 ⁴NCAS climate, University of Cambridge, Cambridge, CB2 1EW, UK

11 ⁵State University of Amazonas, Av. Darcy Vargas, 1200, 69065-020, Manaus-AM, Brazil

12 ⁶Instituto Nacional de Pesquisas da Amazônia (INPA), Clima e Ambiente (CLIAMB),
13 Manaus-AM, Brazil

14 ⁷Department of Earth System Science, University of California, Irvine CA 92697, USA

15 ⁸NOAA ESRL Chemical Sciences Division, Boulder CO, USA.

16 ⁹National Institute of Environmental Research, Republic of Korea

17 ¹⁰Pacific Northwest National Laboratory, Richland WA, USA

18 ¹¹Atmospheric Chemistry Division, National Center for Atmospheric Research, Boulder CO,
19 USA

20 ¹²Dept of Chemistry, University of California, Irvine CA, USA

21 ¹³Sch. Eng. & Appl. Sci., Harvard University, Cambridge, MA 02138 USA

22 ¹⁴Dep. Earth & Planetary Sciences, Harvard University, Cambridge, MA 02138 USA

23

24 *Corresponding authors: I. Kourtchev (ink22@cam.ac.uk) and M. Kalberer
25 (mk594@cam.ac.uk)

26

27

28

29

30

31

32



33 **Abstract**

34 The Amazon basin plays key role in atmospheric chemistry, biodiversity and climate change.
35 In this study we applied nanoelectrospray (nanoESI) ultrahigh resolution mass spectrometry
36 (UHR-MS) for the analysis of the organic fraction of PM_{2.5} aerosol samples collected during
37 dry and wet seasons at a site in central Amazonia receiving background air masses, biomass
38 burning and urban pollution. Comprehensive mass spectral data evaluation methods (e.g.,
39 Kendrick Mass Defect, Van Krevelen diagrams, carbon oxidation state and aromaticity
40 equivalent) were used to identify compound classes and mass distributions of the detected
41 species. Nitrogen and/or sulfur containing organic species contributed up to 60% of the total
42 identified number of formulae. A large number of molecular formulae in organic aerosol (OA)
43 were attributed to later-generation nitrogen- and sulfur-containing oxidation products,
44 suggesting that OA composition is affected by biomass burning and other, potentially
45 anthropogenic, sources. Isoprene derived organo sulfate (IEPOX-OS) was found as the most
46 dominant ion in most of the analysed samples and strongly followed the concentration trends
47 of the gas-phase anthropogenic tracers confirming its mixed anthropogenic-biogenic origin.
48 The presence of oxidised aromatic and nitroaromatic compounds in the samples suggested a
49 strong influence from biomass burning especially during the dry period. Aerosol samples from
50 the dry period and under enhanced biomass burning conditions contained a large number of
51 molecules with high carbon oxidation state and an increased number of aromatic compounds
52 compared to that from wet. The results of this work demonstrate that the studied site is
53 influenced not only by biogenic emissions from forest but also by biomass burning and
54 potentially other anthropogenic emissions from the neighboring urban environments.

55 **Keywords:** organic aerosol, ultra-high resolution mass spectrometry, molecular
56 composition, IEPOX-OS, Amazon.

57

58

59



60 Introduction

61 The Amazon basin plays key role in atmospheric chemistry, biodiversity and climate change
62 (Keller et al., 2009; Andrea et al., 2015). The Amazon rainforest is an important source of
63 Biogenic Volatile Organic Compound (BVOC) emissions to the atmosphere (Greenberg et al.,
64 2004; Alves et al., 2015), which give rise to secondary organic aerosol (SOA) through reaction
65 with atmospheric oxidants (i.e. O_3 , OH and NO_3) (e.g., Martin et al., 2010). SOA particles
66 scatter and absorb solar and terrestrial radiation, influence cloud formation, participate in
67 heterogeneous chemical reactions in the atmosphere, and thus are suggested to play an
68 important role in climate change (Andreae and Crutzen, 1997; Haywood and Boucher, 2000;
69 Hallquist et al., 2009; Pöschl et al., 2010). Aerosol optical properties, which govern the ability
70 to absorb solar radiation, strongly depend on SOA composition, precursor and oxidant types
71 (Laskin et al., 2015). It has been shown that organic nitrates, nitrooxy-organosulfates and
72 organic sulfates may contribute to light absorption by SOA (e.g., Song et al., 2013; Jacobson,
73 1999; Lu et al., 2011; Laskin et al., 2015). Chemical interactions between anthropogenic and
74 biogenic aerosol precursors can play a significant role in the formation of SOA (Goldstein et
75 al., 2009; Hoyle et al., 2011; Kleinman et al., 2015). For example, anthropogenic nitrogen
76 oxides (NO_x) and sulfur dioxide (SO_2) are shown to react with a range of BVOCs leading to
77 formation of organic nitrates (e.g., Roberts, 1990; Day et al., 2010; Fry et al., 2014), nitroxy-
78 organosulfates and organosulfates (Surratt et al., 2008; Budisulistiorini et al., 2015). Much
79 remains to be explored in terms of the molecular diversity of these compounds in the
80 atmosphere.

81 A comprehensive knowledge of aerosol molecular composition, which in turn leads to better
82 understanding of aerosol sources, is required for the development of effective air pollution
83 mitigation strategies. However, identification of the organic aerosol composition, remains a
84 major analytical challenge (Noziere et al., 2015). Organic aerosol is composed of thousands
85 of organic compounds, which cover a wide range of physical and chemical properties
86 (Goldstein and Galbally, 2007) making it difficult to find a single analytical technique for a



87 detailed chemical analysis at the molecular level. Methods based on ultrahigh resolution mass
88 spectrometry (UHRMS) have shown great potential in solving this longstanding problem.
89 UHRMS (e.g., Fourier transform ion cyclotron resonance MS and Orbitrap MS) have a mass
90 resolution power that is at least one order of magnitude higher ($\geq 100\,000$) than conventional
91 MS and high mass accuracy (< 5 ppm) and thus, when coupled with soft ionisation techniques
92 (e.g., electrospray ionisation (ESI)), can provide a detailed molecular composition of the
93 organic aerosol (Nizkorodov et al., 2011; Noziere et al., 2015). Direct infusion ESI-UHRMS
94 has been applied successfully for the analysis of aerosol samples from remote (e.g., boreal
95 forest in Finland, Pico Island of the Azores archipelago), rural (e.g., Millbrook, USA; Harcum,
96 USA; K-Puszt, Hungary) and urban (e.g., Cambridge, UK, Birmingham, UK, Cork, Ireland,
97 Shanghai China and Los Angeles, USA) locations (Wozniak et al., 2008; Schmitt-Kopplin et
98 al., 2010; Kourtchev et al., 2013; 2014; Tao et al., 2014; Dzepina et al., 2015). This technique
99 is extremely useful in assessing chemical properties of the SOA.

100 The aim of this study was to investigate the detailed molecular composition of organic aerosol
101 from a site that received air masses from a wide range of origins, including the background
102 atmosphere of Amazonia, biomass burning and urban pollution plumes. The measurements
103 were performed as a part of the *Observations and Modeling of the Green Ocean Amazon*
104 (GoAmazon2014/5) campaign (Martin et al., 2015). The location of the research site where
105 aerosol was collected for this study is 70 km downwind of Manaus (population 2 million),
106 intersected background and polluted air with day-to-day variability in the position of the
107 Manaus plume. The study designed served as a laboratory for investigating anthropogenic
108 perturbations to biogenic processes and atmospheric chemistry.

109 **Methods**

110 **Sampling site**

111 Aerosol sampling was conducted at site “T3” of GoAmazon2014/5 located at -3.2133° and -
112 60.5987° . $35'55\,32''$ W. The T3 site is located in the pasture area, ~ 2.5 km from the rainforest.



113 The air masses arriving to the sampling site often passed over the single large city in the
114 region. Detailed descriptions of the site and instrumentation are provided in Martin et al.
115 (2015).

116 PM_{2.5} aerosol samples were collected on 47 mm polycarbonate filters Nuclepore, using a
117 Harvard impactor (Air Diagnostics, Harrison, ME, EUA) with flow rate of 10 L min⁻¹ from 5 to
118 26 March 2014 and 5 Sept to 04 Oct of 2014, which were during Intensity Operating Periods
119 1 and 2 (IOP1 and IOP2) of GoAmazon2014/5, respectively, corresponding to the traditional
120 periods of wet and dry seasons of Amazonia. The sampling durations are shown in the Table
121 SI1. The airflow through the sampler was approximately 10 L min⁻¹ for about 24-36 h per
122 sample. After collection, the aerosol samples were transferred into Petri dishes and stored at
123 -4°C until analysis.

124 **Aerosol Sample Analysis**

125 Fifteen samples, 5 from IOP2 and 10 from IOP1, were extracted and analysed using a
126 procedure described elsewhere (Kourtchev et al., 2014; Kourtchev et al., 2015). Briefly, ½ of
127 filters were in methanol (Optima grade, Fisher Scientific) in a chilled ice slurry, filtered through
128 a Teflon filter (0.2 µm, ISODisc™ Supelco), and reduced by volume to approximately 200 µL.
129 The sample was divided into two parts for direct infusion and LC/MS analyses. The LC/MS
130 portion was further evaporated to 20 µL and diluted to 100 µL by aqueous solution of formic
131 acid (0.1%). The final extracts were analysed as described in Kourtchev et al. (2013) using a
132 high-resolution LTQ Orbitrap Velos mass spectrometer (Thermo Fisher, Bremen, Germany)
133 equipped with ESI and a TriVersa Nanomate robotic nanoflow chip-based ESI (Advion
134 Biosciences, Ithaca NY, USA) sources. The Orbitrap MS was calibrated using an Ultramark
135 1621 solution (Sigma-Aldrich, UK). The mass accuracy of the instrument was below 1 ppm.
136 The instrument mass resolution was 100 000 at *m/z* 400. The ion transmission settings were
137 optimised using a mixture of camphor sulfonic acid (20 ng µL⁻¹) glutaric acid (30 ng µL⁻¹), and
138 *cis*-pinonic acid (30 ng µL⁻¹) in methanol and Ultramark 1621 solution. The ionisation voltage



139 and back pressure of the nanoESI direct infusion source were set at -1.4 kV and 0.8 psi,
140 respectively. The inlet temperature was 200 °C and the sample flow rate was approximately
141 200–300 nL min⁻¹. The negative ionisation mass spectra were collected in three replicates at
142 two mass ranges (m/z 100–650 and m/z 150–900) and processed using Xcalibur 3.1 software
143 (Thermo Fischer Scientific Inc.). Similar to our preceding studies (Kourtchev et al., 2015) the
144 average percentage of common peaks between analytical replicates was ~80%. This is also
145 in agreement with literature reports for similar data analysis (Sleighter et al., 2012). LC-MS
146 ESI parameters were as follows: spray voltage -3.6 kV; capillary temperature 300 °C; sheath
147 gas flow 10 arbitrary units, auxiliary gas flow 10; sweep gas flow rate 5; S-lens RF level 58 %.
148 LC/(-)ESI-MS analysis was performed using an Accela system (Thermo Scientific, San Jose,
149 USA) coupled with LTQ Orbitrap Velos MS and a T3 Atlantis C18 column (3 µm; 2.1 x 150
150 mm; Waters, Milford, USA). The sample extracts were injected at a flow rate of 200 µL min⁻¹.
151 The mobile phases consisted of 0.1% formic acid (v/v) (A) and methanol (B). The applied
152 gradient was as follows: 0–3 min 3% B, 3–25 min from 3 to 50% B (linear), 25–43 min from
153 50 to 90% B (linear), 43–48 min from 90 to 3% B (linear), and kept for 12 min at 3% B. The
154 CID settings for MSMS analysis are reported in Kourtchev et al (2015). The identification of
155 IEPOX organosulfates was performed by comparing MS fragmentation patterns and
156 chromatographic elution with a synthesised IEPOX-OS standard which was provided by Dr
157 Surratt from University of North Carolina. It must be noted that due to competitive ionisation
158 of analytes in the direct infusion ESI analysis of the samples with a very complex matrix (i.e.,
159 aerosol extracts), the ion intensities do not directly reflect the concentration of the molecules
160 in the sample; therefore, data shown in this work is semi-quantitative.

161 **High resolution MS data analysis**

162 The direct infusion data analysis was performed using procedures described in detail by
163 Kourtchev et al. (2013). Briefly, for each sample analysis, 60–90 mass spectral scans were
164 averaged into one mass spectrum. Molecular formulae assignments were made using
165 Xcalibur 3.1 software using the following constraints $^{12}\text{C} \leq 100$, $^{13}\text{C} \leq 1$, $^1\text{H} \leq 200$, $^{16}\text{O} \leq 50$, $^{14}\text{N} \leq 5$,



166 $^{32}\text{S} \leq 2$, $^{34}\text{S} \leq 1$. The data processing was performed using a Mathematica 8.0 (Wolfram
167 Research Inc., UK) code developed in-house that utilises a number of additional constraints
168 described in previous studies (Kourtchev et al., 2013; Kourtchev et al., 2015). Only ions that
169 appeared in all three replicates were kept for evaluation.

170 The Kendrick Mass Defect (KMD) is calculated from the difference between the nominal mass
171 of the molecule and the exact KM (Kendrick, 1963). Kendrick mass of the CH_2 unit is calculated
172 by renormalising the exact IUPAC mass of CH_2 (14.01565) to 14.00000.

173 **Benzene and isoprene measurements**

174 For benzene and isoprene analysis we used a high-resolution selective-reagent-ionisation
175 proton transfer reaction time-of-flight mass spectrometer (SRI-PTR-TOF-MS 8000, Ionicon
176 Analytik, Austria). A description of the PTR-TOF-MS instrument and the data reduction
177 process used are provided elsewhere (Graus et al. 2010; Müller et al. 2013). Background of
178 the instrument was measured regularly by passing ambient air through a platinum catalyst
179 heated to 380 °C. Sensitivity calibrations were performed by dynamic dilution of VOCs using
180 several multi-component gas standards (Apel Riemer Environmental Inc., Scott-Marrin, and
181 Air Liquide, USA). The calibration cylinders contained acetaldehyde, acetone, benzene,
182 isoprene, α -pinene, toluene and trichlorobenzene, among others. During IOP1, the instrument
183 was operated with H_3O^+ reagent ion and at a drift tube pressure of 2.3 mbar, voltage of 600
184 V, and temperature of 60 °C, corresponding to an E/N ratio of 130 Td (E being the electric field
185 strength and N the gas number density; 1 Td = 10^{-17} V cm⁻²). During IOP2, the reagent ion
186 was NO^+ and the drift tube settings were 2.3 mbar, 350 V, and 60 °C, resulting in an E/N ratio
187 of 76 Td. The sampling was done with 1 min time resolution and the instrument detection limit
188 for benzene and isoprene were below 0.02 and 0.04 ppbv, respectively.

189 **Air mass history analysis**

190 Air mass history analysis was done for the sampling period using the Numerical Atmospheric-
191 dispersion Modeling Environment (NAME) model, developed by the UK Met Office (Maryon et



al., 1991). NAME is a Lagrangian model in which particles are released into 3D wind fields from the operational output of the UK Met Office Unified Model meteorology data (Davies et al., 2005). These winds have a horizontal resolution of 17 km and 70 vertical levels up that reach ~80 km. In addition, a random walk technique was used to model the effects of turbulence on the trajectories (Ryall and Maryon, 1998). To allow the calculation of air mass history for the average sampling time (which varied between samples, 24, 36 or 48 hours), 10 000 particles per hour were released continuously from the T3 site. The trajectories travelled back in time for 3 days with the position of the particles in the lowest 100 m of the model atmosphere recorded every 15 min. The particle mass below 100 m was integrated over the 72 h travel time. The air mass history ('footprints') for the periods of the analysed filters are shown in Figure S11. The majority of the three-day air mass footprints originated from the east, although wind direction showed variability nearer to the sampling site on some occasions e.g., sample MP14-17 (Fig. S11). Almost all air masses pass over Manaus and therefore highlight this city as a potential source. Some air masses also pass over Manacapuru, but this is rare and the corresponding time-integrated concentrations are lower than the equivalent Manaus values.

Results and discussions

Figure 1 shows mass spectra from two typical samples collected during IOP1 and IOP2. The majority of the ions were associated with molecules below 500 Da. Although ESI is a 'soft' ionisation technique resulting in minimal fragmentation, we cannot exclude the possibility that some of the detected ions correspond to fragments, also in light of the many relative fragile compounds that constitute OA. The largest group of identified number of molecular formulae in all samples were attributed to molecules containing CHO atoms only (1051 ± 141 during IOP2 and 820 ± 139 during IOP1), followed by CHON (537 ± 71 during IOP2 and 329 ± 71 during IOP1), CHOS (183 ± 34 during IOP2 and 137 ± 31 during IOP1) and CHONS (37 ± 11 during IOP2 and 28 ± 10 during IOP1) (Fig. 2). The number of molecular formulae containing CHO and CHON subgroups increased by ~20% from IOP1 to IOP2 period; however, rather insignificant



increase was observed for CHOS and CHONS subgroups. This is consistent with the observed increase in odd reactive nitrogen species (NO_y) from IOP1 to IOP2 (Table SI1). Organic nitrates are believed to form in polluted air through reaction with nitrogen oxides during day and from reaction of NO₃⁻ with BVOCs during nighttime (Day et al., 2010; Ayres et al., 2015). The average concentration of NO_y during IOP1 was found to be on almost two times higher, which is possibly reflected in the increased number of organonitrates in the aerosol samples from IOP2. Moreover, the increase in the number of organonitrates during IOP2 is consistent with the recent studies, which demonstrated that organonitrates groups in aerosol particles may hydrolyse under high RH conditions (Liu et al., 2012). In this respect, while night time RH during both periods was very similar (~90%), day-time RH during IOP1 was higher (89%) compared to that from the 'dry' period (66%) (Fig. SI2).

Carbon oxidation state (OS_C) introduced by Kroll et al. (2011) can be used to describe the composition of a complex mixture of organics undergoing oxidation processes. OS_C was calculated for each molecular formula identified in the mass spectra using the following equation:

$$OS_C = -\sum_i OS_i \frac{n_i}{n_C} \quad (\text{Eq. 1})$$

where OS_i is the oxidation state associated with element i, n_i/n_C is the molar ratio of element i to carbon within the molecule (Kroll et al., 2011).

Figure 3 shows overlaid OS_C plots for two samples from IOP1 and IOP2. Consistent with previous studies, the majority of molecules in the sampled organic aerosol had OS_C between -1.5 and +1 with up to 30 (nC) carbon atoms throughout the selected mass range (*m/z* 100-650) (Kroll et al., 2011 and the references therein). The molecules with OS_C between -1 and +1 with 13 or less carbon atoms (nC) are suggested to be associated with semivolatile and low-volatility oxidised organic aerosol (SV-OOA and LV-OOA) produced by multistep oxidation reactions. The molecules with OS_C between -0.5 and -1.5 with 7 or more carbon atoms are associated with primary biomass burning organic aerosol (BBOA) directly emitted into the



245 atmosphere (Kroll et al., 2011). The cluster of molecules with OSc between -1 and -1.5 and
246 nC less than 10 could be possibly associated with OH radical oxidation products of isoprene
247 (Kourtchev et al., 2015), which is an abundant VOC in Amazon rain forest (Rasmussen and
248 Khalil, 1988; Chen et al., 2015). The isoprene daytime average was above 1.5 ppbv during
249 both seasons, with hourly campaign-averages reaching up to 2.3 and 3.4 ppbv for IOP1 and
250 IOP2, respectively. In general, aerosol samples from IOP1 contained less oxidised molecules
251 compared to those from IOP2. Wet deposition of aged or processed aerosol during wet (i.e.,
252 IOP 2) sampling period cannot be the only reason for the observed differences in OSc. It has
253 been shown that different oxidation regimes to generate SOA (e.g., OH radical vs. ozonolysis)
254 can result in significantly different OSc of SOA (Kourtchev et al., 2015). For example, the SOA
255 component from OH initiated oxidation of α -pinene as well as BVOC mixtures had a molecular
256 composition with higher OSc throughout the entire molecular mass range (Kourtchev et al.,
257 2015) compared to that obtained from ozonolysis reaction.

258 Figure 4 shows the distribution of ion intensities for selected tentatively identified tracer
259 compounds for anthropogenic, biogenic and mixed sources in all 15 samples. The structural
260 or isomeric information is not directly obtained from the direct infusion analysis; therefore, the
261 identification of the tracer compounds was achieved by comparing MSMS fragmentation
262 patterns from authentic standards and published literature. The tracer compounds include
263 anhydrosugars, structural isomers with a molecular formula $C_6H_{10}O_5$ at m/z 161.0456
264 corresponding to levoglucosan, mannosan, galactosan and 1,6-anhydro- β -D-glucofuranose,
265 which are regarded as marker compounds for biomass burning (Simoneit et al., 1999;
266 Pashynska et al., 2002; Kourtchev et al., 2011). Nitrocatechols, with a molecular formula
267 $C_6H_5NO_4$ at m/z 154.01458, are attributed to mixed anthropogenic sources, e.g., biomass and
268 vehicular emissions sources. 3-methyl-1,2,3-butanetricarboxylic acid (3-MBTCA), with a
269 molecular formula $C_8H_{12}O_6$ at m/z 203.05611, is an OH-initiated oxidation product of α - and β -
270 pinene (Szmigielski et al., 2007), and regarded as a tracer for processed or biogenic SOA.
271 Finally, isoprene epoxydiol organosulfate ester (IEPOX-OS), with a molecular formula



272 $C_5H_{12}O_7S$ at m/z 215.0231, is shown in Figure 4. From studies in mid latitude environments it
273 has been suggested that IEPOX-OS is formed through reactions between SO_x and isoprene
274 oxidation products (Pye et al., 2013; Budisulistiorini et al., 2015) and thus can be used to
275 observe the extent of SO₂ aging effects on the biogenic SOA. Direct infusion analysis suffers
276 from competitive ionisation in the complex matrices and thus comparing ion intensities across
277 samples has to be done with caution. Nevertheless, all selected tracers showed very similar
278 variations with benzene concentration that was measured in the gas-phase using PTR-MS
279 (Fig. 3). Benzene, generally regarded as an anthropogenic species, has various sources
280 including industrial solvent production, vehicular emissions and biomass burning (Hsieh et al.,
281 1999; Seco et al., 2013; Friedli et al., 2001). Recent studies indicated that vegetation (leaves,
282 flowers, and phytoplankton) emits a wide variety of benzenoid compounds to the atmosphere
283 at substantial rates (Misztal et al., 2015). However, considering that benzene concentration
284 correlated very well with another anthropogenic tracer CO ($R^2=0.77$, Figure SI3) during IOP1
285 and IOP2 periods, it is rather likely that the observed benzene concentrations were mainly due
286 to anthropogenic emissions. During the sampling period, irrespectively of the season, air
287 masses passed over the large city Manaus and small municipalities located near the T3 site
288 (Figure SI1). It must be noted that due to rather low sampling resolution time ($\geq 24h$) the
289 molecular composition of all analysed samples is likely to be influenced by clean air masses
290 and anthropogenic plumes from these urban locations which usually last only a few hours per
291 day and thus individual urban plume events cannot be identified with the data analysed here.
292 During IOP1 much lower incidents of forest fires were observed compared to that during IOP2
293 (Martin et al., 2016). For example, a number of forest fires in the radius of 200 km from the
294 sampling site varied between 0 to 340 fires (<http://www.dpi.inpe.br/proarco/bdqueimadas/>).
295 This is reflected in the ion intensities of the particle phase biomass burning markers, i.e.,
296 anhydrosugars ($C_6H_{10}O_5$) and nitrocatechols ($C_6H_5NO_4$) and gas-phase benzene
297 concentrations, which were significantly lower during IOP1 compared to that from IOP2, when
298 on average more fires are observed.



299 It should be noted that ion intensities for anhydrosugars ($C_6H_{10}O_5$) and nitrocatechols
300 ($C_6H_5NO_4$) showed very good correlation ($R^2 > 0.7$) suggesting that nitrocatechols, observed
301 at the sampling site, are mainly associated with biomass burning sources. The highest ion
302 intensities of these tracer compounds were observed during two periods: 7-9 September 2014
303 (sample MP14-128) and 27-28 September 2014 (sample MP14-148) with the later one
304 coinciding with highest incident of fires (340 fires). Although during 7-9 September (sample
305 MP14-128) a significantly lower number (22 fires) of fires was observed compared to the
306 period of 27-28 September 2014, lower wind speed occurring during 7-9 September suggests
307 that high intensity of the biomass burning markers could be due to the biomass burning
308 emissions from nearby sources. Between the T3 sampling site and Manaus (about 20 km east
309 of the site), there are a number of small brick factories, which use wood to fire the kilns (Martin
310 et al., 2016) and thus they are an additional local wood burning source besides the forest and
311 pasture fires.

312 Interestingly the sample MP14-148 had the highest ion intensity corresponding to IEPOX-OS
313 (Fig. 4), which also coincided with the strong increase of the ion intensity at m/z 96.95987
314 corresponding $[HSO_4^-]$. This is consistent with organosulfates formation mechanism through
315 reactive uptake of isoprene epoxydiols (IEPOX) in the presence of acidic sulfate seed (Surratt
316 et al., 2010; Lin et al., 2012; 2013). A similar relationship between sulfate and organosulfates
317 concentrations has been observed previously in field studies in the Southeastern US (Surratt
318 et al., 2007, 2008, 2010; Lin et al., 2012, 2013). It should be noted that the 27-28 September
319 period (sample MP14-148) was marked by a very strong increase in the CO concentration
320 (Fig. SI4). In mid-latitude environments it has been suggested that the production of
321 anthropogenic SOA in an air mass, as it travels from an urban source region, can be estimated
322 by using a relatively inert pollution tracer, such as CO occurring in the air mass (De Gouw et
323 al., 2005; Hoyle et al., 2011). At T3 sampling site, highest CO concentrations are observed in
324 air masses affected by biomass burning. Therefore, it is possible that organic aerosol in the



sample MP14-148 has experienced the highest contribution from biomass burning as well as other anthropogenic activities.

To investigate the influence of anthropogenic activities (i.e., biomass burning) on a detailed molecular composition of organic aerosol at the T3 site we compared samples from the periods with the lowest (9 fires), moderately high (254 fires) and the highest (340 fires) incidents of fires occurring within 200 km around the site.

Figure 5 (a-c) shows H/C ratios of CHO containing formulae as a function of their molecular mass and double bond equivalent (DBE), which shows a degree of unsaturation of the molecule, for a sample with the lowest (a) moderately high (b) and highest incidents (c) of fires. One of the obvious differences between these samples is the abundance of ions with low H/C ratios (< 1). The majority of these ions have DBE above 7 indicating that they likely correspond to oxidised aromatic compounds, which are mainly of anthropogenic origin (Kourtchev et al., 2014; Tong et al., 2016). For example, the smallest polycyclic aromatic hydrocarbon (PAH), naphthalene with a molecular formulae $C_{10}H_8$ has an $H/C=0.8$ and $DBE=7$. The number of CHO containing formulae with high DBE equivalent and low H/C increased dramatically during the days with moderately high and high incidents of fires (Fig. 5a-c), suggesting that they are mainly associated with biomass burning.

Recent studies indicated that different families of compounds with heteroatoms (e.g. O, S) overlap in terms of DBE and thus may not accurately indicate the level of unsaturation of organic compounds. For example, the divalent atoms, such as oxygen and sulphur, do not influence the value of DBE, yet they may contribute to the potential double bonds of that molecule (Reemtsma 2009; Yassine et al., 2014). Yassine et al (2014) suggested using aromaticity equivalent (X_c), to improve the identification and characterisation of aromatic and condensed aromatic compounds in WSOC. The aromaticity equivalent can be calculated as follows:

$$X_c = \frac{3(DBE - (mN_O + nN_S)) - 2}{DBE - (mN_O + nN_S)} \quad (\text{Eq. 2})$$



351 where 'm' and 'n' correspond to a fraction of oxygen and sulfur atoms involved in π -bond
352 structures of a compound, which varies depending on the compound class. For example,
353 carboxylic acids, esters, and nitro functional groups have $m=n=0.5$. For compounds containing
354 functional groups such as aldehydes, ketones, nitroso, cyanate, alcohol, or ethers 'm' and 'n'
355 are 1 or 0. Considering that ESI, in negative mode, is most sensitive to compounds containing
356 carboxylic groups we, therefore, used $m=n=0.5$ for the calculation of the X_c . For molecular
357 formulae with an odd number of oxygen or sulfur, the sum (mN_O+nN_S) in Eq. 2 was rounded
358 down to the closest integer as detailed in Yassine et al (2014). The authors proposed that
359 aromaticity equivalent with $X_c \geq 2.50$ and $X_c \geq 2.71$ as unambiguous minimum criteria for the
360 presence of aromatics and condensed aromatics.

361 Expressing our data using aromaticity equivalents confirmed that the increase in the number
362 of molecules with high DBE from the sample with the lowest to the highest incidents of fires
363 was due to the increase in the number of aromatic and condensed aromatic compounds in the
364 aerosol samples (Figures SI5). Considering the Yassine et al. (2014) assignment criteria for
365 the aromatic-reach matrices, the highest number of the aromatic compounds in the Amazon
366 samples was observed for formulae with a benzene core structure ($X_c = 2.50$) followed by
367 formulae with pyrene core structure ($X_c = 2.83$), and an ovalene core structure ($X_c = 2.92$) as
368 well as highly condensed aromatic structures or highly unsaturated compounds ($X_c > 2.93$).

369 Interestingly, a similar trend was observed for the molecules containing CHON subgroups
370 (Figure SI6). A number of CHON molecules with low H/C (<1) and high DBE (≥ 5) almost
371 doubled from the days with 9 to 340 fires (Figure SI7). Nitroaromatic compounds, such as
372 nitrophenols (DBE=5) and N-heterocyclic compounds are often observed in the PM from the
373 biomass burning sources (Kitanovski et al., 2012a,b) and have been suggested as potential
374 contributors to light absorption by brown carbon (Laskin et al., 2015). The differences in the
375 increased number of nitroaromatic compounds in aerosol samples affected by biomass
376 burning are also apparent in overplayed Van Krevelen diagrams (Figure 6), which show H/C
377 and O/C ratios for each formula in a sample. Van Krevelen diagrams, can be used to describe



the overall composition or evolution of organic mixtures (Van Krevelen, 1993; Nizkorodov et al., 2011; Noziere et al., 2015). Organic aerosol affected by biomass burning contained significantly larger number of CHON formulae with $O/C < 0.5$ and $H/C < 1$ (Fig. 6a and b, area B) but smaller number of formulae with $O/C < 0.5$ and $H/C > 1$. (Fig. 6a and b, area A). While molecules with H/C ratios (<1.0) and O/C ratios (<0.5) (area A in Fig. 3) are generally associated with aliphatic compounds typically belong to oxidised aromatic hydrocarbons, molecules with high H/C ratios (>1.5) and low O/C ratios (<0.5) (area B in Fig. 3) (Mazzoleni et al., 2010; 2012). Although the smaller number of nitro aliphatic compounds in the samples affected by biomass burning requires further investigation, it is possible that they were oxidised in the polluted air by NO_x and O_3 (Zahardis et al., 2009; Malloy et al., 2009), which production is significantly enhanced during fire events (e.g., Galanter et al., 2000). The majority (up to 80%) of the CHON molecules in the analysed samples have O/C ratios < 0.7 (Fig. 6). The relatively low oxygen content suggests that these molecules include reduced nitrogen-containing compounds (Zhao et al., 2013). Although biomass burning material type is expected to result in different molecular composition, the presence of a large number of molecules with low O/C ratio is consistent with the literature. For example, most of the CHON molecules in OA from wheat straw burning in K-puszt, Great Hungarian Plain in Hungary and biomass burning at Canadian rural sites (Saint Anicet, Quebec, and Canterbury, New Brunswick) had O/C ratios below 0.7 (Schmitt-Kopplin et al., 2010).

Figure 7 shows overlaid OSc plots for OA from the days with low, moderately high and high incidents of fires. During the days affected by high and moderately high number of fires, OSc was shifted towards more oxidised state for the CHO molecules containing more than 7 carbon atoms. This difference becomes even more pronounced with the increased number of carbons in the detected molecular formulae. Interestingly, the affected ions with high OSc do not fall into the category of the BBOA (encircled area in Fig. 7) which are associated with primary particulate matter directly emitted into the atmosphere as defined in Kroll et al (2011).



404 At first glance, biomass burning seems to influence the number and intensity of the CHOS
405 containing formulae; however, the effect was at a much lower extent compared to that for the
406 CHO and CHON molecules (see discussion above). Higher number of CHOS containing
407 molecules was observed in the sample (MP14-148) corresponding to the highest incident of
408 fires (Figures 8a). Interestingly, IEPOX-OS was found to be very abundant in the sample that
409 experienced the highest incidents of fires (Figure 8a). The significant IEPOX-OS mass was
410 previously observed during a low-altitude flight campaigns at Northern California and southern
411 Oregon at high NO conditions (> 500 pptv) (Liao et al., 2015). The authors explained this
412 observation by the transport or formation of IEPOX from isoprene hydroxynitrate oxidation
413 (Jacobs et al., 2014) and higher sulphate aerosol concentrations occurring during their
414 sampling period (Nguyen et al., 2014). This explanation is also consistent with our results. The
415 ion at m/z 96.95987 corresponding $[\text{HSO}_4]^-$ in UHR mass spectra of the sample MP14-148
416 was three times more abundant compared that in the sample MP14-129 suggesting that
417 particle acidity may be one of the reasons for the high abundance of the IEPOX-OS in this
418 sample. Considering that the main sources of sulphate at T3 site are industrial pollution (e.g.,
419 power plants), natural and long range-sources, they could also be responsible for the high
420 abundance of the sulphate and IEPOX-OS in the samples besides the overlapping biomass
421 burning event. Noticeably, these samples not only contained a larger number of oxygenated
422 CHOS-containing molecules with $\text{O/C} > 1.2$ but also molecules with $\text{O/C} < 0.6$ and H/C ranging
423 from 0.4 to 2.2. Recent laboratory and field studies indicated the presence of a large number
424 of aromatic and aliphatic OSs and sulfonates in OA and linked them to anthropogenic
425 precursors (Tao et al., 2014; Wang et al., 2015; Riva et al., 2015; 2016; Kuang et al., 2016).
426 Riva et al (2015, 2016) demonstrated formation of OSs and sulfonates in the laboratory smog
427 chamber experiments from photooxidation of alkanes and PAHs, respectively. The authors
428 indicated enhancement of organosulfates yields in the presence of the acidified ammonium
429 sulphate seed and suggested that these OSs are mainly formed through reactive uptake of
430 gas-phase epoxides. It must be noted that above cited field studies are based on



431 measurements at the Northern Hemisphere USA and thus organosulfates formation pathways
432 and sources may differ from that of Amazonia.

433 KMD plots are useful visualisation technique for identification of homologous series of
434 compounds differing only by the number of a specific base unit (e.g., a CH₂ group).
435 Anthropogenically affected aerosol samples have longer homologous series of molecules
436 containing CHOS subgroups (Figure 8b). One of these longer series includes a second most
437 intensive ion at m/z 213.0075 (C₅H₁₀O₇S). The compound with molecular formula C₅H₁₀O₇S
438 has been previously observed in the laboratory and field studies and attributed to isoprene
439 derived organosulfates (Surratt et al., 2008; Gómez-González, 2008; Kristensen and Glassius,
440 2011; Nguyen et al., 2014; Hettiyadura et al., 2015). The KMD plot (Figure 8b) shows that OA
441 from the anthropogenically affected samples contained an additional series of CHOS
442 molecules with high KMD >0.33 that were not present in the sample from the less polluted
443 period. Most of these ions are highly oxygenated (containing >10 oxygens) and are likely to
444 be associate with molecules produced through homogeneous photochemical ageing reactions
445 (Hildebrandt et al., 2010).

446 It is worth noting that in the most of the samples IEPOX-OS was not a part of any homologous
447 series in KMD plot (e.g., Fig 8b). This observation confirms that atmospheric oxidation
448 reactions resulting in the incorporation of S and N functional groups do not always conserve
449 homologous series but could also lead to a wide range of possible reaction products (Rincon
450 et al., 2012; Kourtchev et al., 2013).

451 Conclusions

452 In this study we applied direct infusion nanoESI UHR-MS for the analysis of the organic
453 fraction of PM_{2.5} samples collected IOP1 and IOP2 of GoAmazon2014/5 in central Amazonia
454 which is influenced by both background and polluted air masses. Up to 2100 elemental
455 formulae were identified in the samples, with the largest number of formulae found during
456 IOP2. The distribution of several tracer compounds along with the comprehensive mass



457 spectral data evaluation methods (e.g., Kendrick Mass Defect, Van Krevelen diagrams,
458 carbon oxidation state and aromaticity equivalent) applied to the large UHRMS datasets were
459 used to identify various sources of organic aerosol components, including natural biogenic
460 sources, biomass burning and anthropogenic emissions. The distinguishable homologous
461 series in the KMD diagram contained nitrogen-containing series included NACs, e.g.,
462 nitrocatechols, nitrophenols, nitroguaiacols and nitrosalicylic acids derived from biomass
463 burning material. Isoprene derived IEPOX-OS was found as the most dominant ion in most of
464 the analysed samples and strongly followed the concentration trends of the gas-phase
465 anthropogenic tracer benzene and CO (with biomass burning as dominant tracer at the T3
466 site) supporting its mixed biomass burning-anthropogenic-biogenic origin. Van Krevelen, DBE
467 and Xc distributions along with relatively low elemental O/C and H/C ratios indicated the
468 presence of a large number of oxidised aromatic compounds in the samples. A significant
469 number of CHO containing formulae in aerosol samples from IOP2 had higher oxidation state
470 compared to that from IOP1 and became even more important during the days with the highest
471 incidents of fires. Although our results suggest that the studied site is not only significantly
472 influenced by biogenic emissions and biomass burning but also anthropogenic emissions from
473 the neighboring urban activities, future work is needed to better understand the quantitative
474 contributions of the various factors to the aerosol composition at the T3 site. The analysis of
475 aerosol samples with higher sampling resolution would allow separating these sources in more
476 detail and thus significantly improve the understanding of the aerosol formation sources at the
477 site.

478 **Acknowledgment:**

479 Research at the University of Cambridge was supported by the ERC grant no. 279405. The
480 authors would like to thank Dr Jason Surratt (University of North Carolina) for providing a
481 synthesised IEPOX-OS standard. O₃, CO, NO_y, RH and rain data were obtained from the
482 Atmospheric Radiation Measurement (ARM) Climate Research Facility, a U.S. Department of
483 Energy Office of Science user facility sponsored by the Office of Biological and Environmental



484 Research. We acknowledge the support from the Central Office of the Large Scale Biosphere
485 Atmosphere Experiment in Amazonia (LBA), the Instituto Nacional de Pesquisas da Amazonia
486 (INPA), and the Universidade do Estado do Amazonia (UEA). The work was conducted under
487 001030/2012-4 of the Brazilian National Council for Scientific and Technological Development
488 (CNPq).

489 **References:**

490 Andreae, M. O. and Crutzen, P. J.: Atmospheric aerosols: Biogeochemical sources and role
491 in atmospheric chemistry, *Science*, 276, 1052–1058, 1997.

492 Andreae, M. O., Acevedo, O. C., Araújo, A., Artaxo, P., Barbosa, C. G. G., Barbosa, H. M.
493 J., Brito, J., Carbone, S., Chi, X., Cintra, B. B. L., da Silva, N. F., Dias, N. L., Dias-Júnior, C.
494 Q., Ditas, F., Ditz, R., Godoi, A. F. L., Godoi, R. H. M., Heimann, M., Hoffmann, T.,
495 Kesselmeier, J., Könemann, T., Krüger, M. L., Lavric, J. V., Manzi, A. O., Lopes, A. P.,
496 Martins, D. L., Mikhailov, E. F., Moran-Zuloaga, D., Nelson, B. W., Nölscher, A. C., Santos
497 Nogueira, D., Piedade, M. T. F., Pöhlker, C., Pöschl, U., Quesada, C. A., Rizzo, L. V., Ro,
498 C.-U., Ruckteschler, N., Sá, L. D. A., de Oliveira Sá, M., Sales, C. B., dos Santos, R. M. N.,
499 Saturno, J., Schöngart, J., Sörgel, M., de Souza, C. M., de Souza, R. A. F., Su, H.,
500 Targhetta, N., Tóta, J., Trebs, I., Trumbore, S., van Eijck, A., Walter, D., Wang, Z., Weber,
501 B., Williams, J., Winderlich, J., Wittmann, F., Wolff, S., and Yáñez-Serrano, A. M.: The
502 Amazon Tall Tower Observatory (ATTO): overview of pilot measurements on ecosystem
503 ecology, meteorology, trace gases, and aerosols, *Atmos. Chem. Phys.*, 15, 10723-10776,
504 2015.

505 Alves, E. G., Jardine, K., Tota, J., Jardine, A., Yáñez-Serrano, A. M., Karl, T., Tavares, J.,
506 Nelson, B., Gu, D., Stavrakou, T., Martin, S., Manzi, A., and Guenther, A.: Seasonality of
507 isoprenoid emissions from a primary rainforest in central Amazonia, *Atmos. Chem. Phys.*
508 *Discuss.*, 15, 28867-28913, 2015.

509 Ayres, B. R., Allen, H. M., Draper, D. C., Brown, S. S., Wild, R. J., Jimenez, J. L., Day, D. A.,
510 Campuzano-Jost, P., Hu, W., de Gouw, J., Koss, A., Cohen, R. C., Duffey, K. C., Romer, P.,
511 Baumann, K., Edgerton, E., Takahama, S., Thornton, J. A., Lee, B. H., Lopez-Hilfiker, F. D.,
512 Mohr, C., Wennberg, P. O., Nguyen, T. B., Teng, A., Goldstein, A. H., Olson, K., and Fry, J.
513 L.: Organic nitrate aerosol formation via NO_3 + biogenic volatile organic compounds in the
514 southeastern United States, *Atmos. Chem. Phys.*, 15, 13377-13392, 2015.

515 Budisulistiorini, S. H., Li, X., Bairai, S. T., Renfro, J., Liu, Y., Liu, Y. J., McKinney, K. A.,
516 Martin, S. T., McNeill, V. F., Pye, H. O. T., Nenes, A., Neff, M. E., Stone, E. A., Mueller, S.,
517 Knote, C., Shaw, S. L., Zhang, Z., Gold, A., and Surratt, J. D.: Examining the effects of
518 anthropogenic emissions on isoprene-derived secondary organic aerosol formation during
519 the 2013 Southern Oxidant and Aerosol Study (SOAS) at the Look Rock, Tennessee ground
520 site, *Atmos. Chem. Phys.*, 15, 8871-8888, 2015.



- 521 Chen, Q., Farmer, D. K., Rizzo, L. V., Pauliquevis, T., Kuwata, M., Karl, T. G., Guenther, A.,
522 Allan, J. D., Coe, H., Andreae, M. O., Pöschl, U., Jimenez, J. L., Artaxo, P., and Martin, S.
523 T.: Submicron particle mass concentrations and sources in the Amazonian wet season
524 (AMAZE-08), Atmos. Chem. Phys., 15, 3687-3701, 2015.
- 525 Davies, T., Cullen, M. J. P., Malcolm, A. J., Mawson, M. H., Staniforth, A., White, A. A., and
526 Wood, N.: A new dynamical core for the Met Office's global and regional modelling of the
527 atmosphere, Q. J. Roy. Meteorol. Soc., 131, 1759–1782, 2005.
- 528 Day, D. A., Liu, S., Russell, L. M. and Ziemann, P. J.: Organonitrate group concentrations in
529 submicron particles with high nitrate and organic fractions in coastal southern California,
530 Atmos. Environ., 44, 1970-1979, 2010.
- 531 de Gouw, J. A., Middlebrook, A. M., Warneke, C., Goldan, P. D., Kuster, W. C., Roberts, J.
532 M., Fehsenfeld, F. C., Worsnop, D. R., Canagaratna, M. R., Pszenny, A. A. P., Keene, W.
533 C., Marchewka, M., Bertman, S. B., and Bates, T. S.: Budget of organic carbon in a polluted
534 atmosphere: Results from the New England Air Quality Study in 2002, J. Geophys. Res.-
535 Atmos., 110, D16305, doi:10.1029/2004jd005623, 2005.
- 536 Dzepina, K., Mazzoleni, C., Fialho, P., China, S., Zhang, B., Owen, R. C., Helmig, D.,
537 Hueber, J., Kumar, S., Perlinger, J. A., Kramer, L. J., Dziobak, M. P., Ampadu, M. T., Olsen,
538 S., Wuebbles, D. J., and Mazzoleni, L. R.: Molecular characterization of free tropospheric
539 aerosol collected at the Pico Mountain Observatory: a case study with a long-range
540 transported biomass burning plume, Atmos. Chem. Phys., 15, 5047-5068, 2015.
- 541 Friedli, H. R., E. Atlas, V. R. Stroud, L. Giovanni, T. Campos, and L. F. Radke: Volatile
542 organic trace gases emitted from North American wildfires, Global Biogeochem. Cycles, 15,
543 435–452, 2001.
- 544 Fry, J. L., Draper, D. C., Barsanti, K. C., Smith, J. N., Ortega, J., Winkler, P. M., Lawler, M.
545 J., Brown, S. S., Edwards, P. M., Cohen, R. C., and Lee, L.: Secondary organic aerosol
546 formation and organic nitrate yield from NO₃ oxidation of biogenic hydrocarbons, Environ.
547 Sci. Technol., 48, 11944–11953, 2014.
- 548 Galanter, M., Levy II, H., and Carmichael, G. R.: Impacts of biomass burning on tropospheric
549 CO, NO_x, and O₃, J. Geophys. Res., 105, 6633–6653, 2000.
- 550 Graus, M., Müller, M. and Hansel, A.: High Resolution PTR-TOF: Quantification and Formula
551 Confirmation of VOC in Real Time, J. Am. Soc. Mass Spectrom., 21, 1037-1044, 2010.
- 552 Greenberg, J., Guenther, A., Petron, G., Wiedinmyer, C., Vega, O., Gatti, L. V., Tota, J., and
553 Fisch, G.: Biogenic VOC emissions from forested Amazonian landscapes, Global Change
554 Biol., 10(5), 651–662, 2004.
- 555 Gómez-González, Y., Surratt, J. D., Cuyckens, F., Szmigielski, R., Vermeylen, R., Jaoui, M.,
556 Lewandowski, M., Offenberg, J. H., Kleindienst, T. E., Edney, E. O., Blockhuys, F., Van
557 Alsenoy, C., Maenhaut, W., and Claeys, M.: Characterization of organosulfates from the
558 photooxidation of isoprene and unsaturated fatty acids in ambient aerosol using liquid
559 chromatography/(–) electrospray ionization mass spectrometry, J. Mass Spectrom., 43, 371–
560 382, 2008.



- 561 Goldstein, A. H. and Galbally, I. E.: Known and unexplored organic carbon constituents in
562 the Earth's atmosphere, *Environ. Sci. Technol.*, 41, 1514–1521, 2007.
- 563 Goldstein, A. H., Koven, C. D., Heald, C. L., and Fung, I. Y.: Biogenic carbon and
564 anthropogenic pollutants combine to form a cooling haze over the southeastern United
565 States, *P. Natl. Acad. Sci. USA*, 106, 8835–8840, 2009.
- 566 Hallquist, M., Wenger, J. C., Baltensperger, U., Rudich, Y., Simpson, D., Claeys, M.,
567 Dommen, J., Donahue, N. M., George, C., Goldstein, A. H., Hamilton, J. F., Herrmann, H.,
568 Hoffmann, T., Iinuma, Y., Jang, M., Jenkin, M. E., Jimenez, J. L., Kiendler-Scharr, A.,
569 Maenhaut, W., McFiggans, G., Mentel, Th. F., Monod, A., Prevot, A. S. H., Seinfeld, J. H.,
570 Surratt, J. D., Szmigielski, R., and Wildt, J.: The formation, properties and impact of
571 secondary organic aerosol: current and emerging issues, *Atmos. Chem. Phys.*, 9, 5155–
572 5235, 2009.
- 573 Haywood, J. and Boucher, O.: Estimates of the direct and indirect radiative forcing due to
574 tropospheric aerosols: A review, *Rev. Geophys.*, 38, 513–543, 2000.
- 575 Hildebrandt, L., Engelhart, G. J., Mohr, C., Kostenidou, E., Lanz, V. A., Bougiatioti, A.,
576 DeCarlo, P. F., Prevot, A. S. H., Baltensperger, U., Mihalopoulos, N., Donahue, N. M., and
577 Pandis, S. N.: Aged organic aerosol in the Eastern Mediterranean: the Finokalia Aerosol
578 Measurement Experiment – 2008, *Atmos. Chem. Phys.*, 10, 4167–4186, 2010.
- 579 Hettiyadura, A. P. S., Stone, E. A., Kundu, S., Baker, Z., Geddes, E., Richards, K., and
580 Humphry, T.: Determination of atmospheric organosulfates using HILIC chromatography with
581 MS detection, *Atmos. Meas. Tech.*, 8, 2347–2358, 2015.
- 582 Hoyle, C. R., Boy, M., Donahue, N. M., Fry, J. L., Glasius, M., Guenther, A., Hallar, A. G.,
583 Huff Hartz, K., Petters, M. D., Petaja, T., Rosenoern, T., and Sullivan, A. P.: A review of the
584 anthropogenic influence on biogenic secondary organic aerosol, *Atmos. Chem. Phys.*, 11,
585 321–343, 2011.
- 586 Jacobson, M. Z.: Isolating nitrated and aromatic aerosols and nitrated aromatic gases as
587 sources of ultraviolet light absorption, *J. Geophys. Res. Atmospheres*, 104 (D3), 3527–3542,
588 1999.
- 589 Jacobs, M. I., Burke, W. J., and Elrod, M. K.: Kinetics of the reactions of isoprene-derived
590 hydroxynitrates: Gas phase epoxide formation and solution phase hydrolysis, *Atmos. Chem.*
591 *Phys.*, 14, 8933–8946, 2014.
- 592 Kendrick E.: A Mass Scale Based on $\text{CH}_2 = 14.0000$ for High Resolution Mass Spectrometry
593 of Organic Compounds, *Anal. Chem.*, 35 (13), 2146–2154, 1963.
- 594 Keller, M., Bustamante, M., Gash, J., and Dias, P.: Amazonia and Global Change, Vol. 186,
595 American Geophysical Union, Wiley, Washington, D.C., 2009.
- 596 Kitanovski, Z., Grgić, I., Vermeylen, R., Claeys, M., and Maenhaut, W.: Liquid
597 chromatography tandem mass spectrometry method for characterization of monoaromatic
598 nitro-compounds in atmospheric particulate matter, *J. Chromatogr. A*, 1268, 35–43, 2012a.



- 599 Kitanovski, Z., Grgic, I., Yasmeen, F., Claeys, M., and Cusak, A.: Development of a liquid
600 chromatographic method based on ultraviolet-visible and electrospray ionization mass
601 spectrometric detection for the identification of nitrocatechols and related tracers in biomass
602 burning atmospheric organic aerosol, *Rapid Commun. Mass Sp.*, 26, 793–804, 2012b.
- 603 Kourtchev, I., Hellebust, S., Bell, J. M., O'Connor, I. P., Healy, R. M., Allanic, A., Healy, D.,
604 Wenger, J. C., and Sodeau, J. R.: The use of polar organic compounds to estimate the
605 contribution of domestic solid fuel combustion and biogenic sources to ambient levels of
606 organic carbon and PM_{2.5} in Cork Harbour, Ireland, *Sci.Total Environ.*, 409, 2143–2155,
607 2011.
- 608 Kourtchev, I., Fuller, S., Aalto, J., Ruuskanen, T. M., McLeod, M. W., Maenhaut, W., Jones,
609 R., Kulmala, M., and Kalberer, M.: Molecular composition of boreal forest aerosol from
610 Hyytiälä, Finland, using ultrahigh resolution mass spectrometry, *Environ. Sci. Technol.*, 47,
611 4069–4079, 2013.
- 612 Kourtchev, I., O'Connor, I. P., Giorio, C., Fuller, S., Kristensen, K., Maenhaut, W., Wenger,
613 J. C., Sodeau, J. R., Glasius, M., and Kalberer, M.: Effects of anthropogenic emissions on
614 the molecular composition of urban organic aerosols: an ultrahigh resolution mass
615 spectrometry study, *Atmos. Environ.*, 89, 525–532, 2014.
- 616 Kourtchev, I., Doussin, J.-F., Giorio, C., Mahon, B., Wilson, E. M., Maurin, N., Pangui, E.,
617 Venables, D. S., Wenger, J. C., and Kalberer, M.: Molecular composition of fresh and aged
618 secondary organic aerosol from a mixture of biogenic volatile compounds: a high-resolution
619 mass spectrometry study, *Atmos. Chem. Phys.*, 15, 5683–5695, 2015.
- 620 Kristensen, K. and Glasius, M.: Organosulfates and oxidation products from biogenic
621 hydrocarbons in fine aerosols from a forest in North West Europe during spring, *Atmos.*
622 *Environ.*, 45, 4546–4556, 2011.
- 623 Kroll, J. H., Donahue, N. M., Jimenez, J. L., Kessler, S. H., Canagaratna, M. R., Wilson, K.
624 R., Altieri, K. E., Mazzoleni, L. R., Wozniak, A. S., Bluhm, H., Mysak, E. R., Smith, J. D.,
625 Kolb, C. E., and Worsnop, D. R.: Carbon oxidation state as a metric for describing the
626 chemistry of atmospheric organic aerosol, *Nat. Chem. Biol.*, 3, 133–139, 2011.
- 627 Kleinman, L., Kuang, C., Sedlacek, A., Senum, G., Springston, S., Wang, J., Zhang, Q.,
628 Jayne, J., Fast, J., Hubbe, J., Shilling, J., and Zaveri, R.: What do correlations tell us about
629 anthropogenic–biogenic interactions and SOA formation in the Sacramento Plume during
630 CARES?, *Atmos. Chem. Phys. Discuss.*, 15, 25381–25431, 2015.
- 631 Kuang, B.Y., Lin, P., Hub, M., and Yu, J.Z.: Aerosol size distribution characteristics of
632 organosulfates in the Pearl River Delta region, China, *Atmos. Environ.*, 130, 23–35, 2016.
- 633 Laskin, A., Laskin, J., and Nizkorodov, S. A.: Chemistry of Atmospheric Brown Carbon,
634 *Chem. Rev.*, 115, 4335–4382, 2015.
- 635 Liao, J., Froyd, K. D., Murphy, D. M., Keutsch, F. N., Yu, G., Wennberg, P. O., St. Clair, J.
636 M., Crounse, J. D., Wisthaler, A., Mikoviny, T., Jimenez, J. L., Campuzano-Jost, P., Day, D.
637 A., Hu, W., Ryerson, T. B., Pollack, I. B., Peischl, J., Anderson, B.E., Ziemba, L. D., Blake,
638 D. R., Meinardi, S., and Diskin, G.: Airborne measurements of organosulfates over the
639 continental U. S., *J. Geophys. Res.*, 120, 2990–3005, doi: 10.1002/2014JD022378, 2015.



- 640 Lin, Y. H., Zhang, Z. F., Docherty, K. S., Zhang, H. F., Budisulistiorini, S. H., Rubitschun, C.
641 L., Shaw, S. L., Knipping, E. M., Edgerton, E. S., Kleindienst, T. E., Gold, A., and Surratt, J.
642 D.: Isoprene Epoxidiols as Precursors to Secondary Organic Aerosol Formation: Acid-
643 Catalyzed Reactive Uptake Studies with Authentic Compounds, *Environ. Sci. Technol.*, 46,
644 250–258, 2012.
- 645 Lin, Y.-H., Knipping, E. M., Edgerton, E. S., Shaw, S. L., and Surratt, J. D.: Investigating the
646 influences of SO₂ and NH₃ levels on isoprene-derived secondary organic aerosol formation
647 using conditional sampling approaches, *Atmos. Chem. Phys.*, 13, 8457–8470, 2013.
- 648 Lu, J. W., Flores, J. M., Lavi, A., Abo-Riziq, A., and Rudich, Y.: Changes in the optical
649 properties of benzo[a]pyrene-coated aerosols upon heterogeneous reactions with NO₂ and
650 NO₃, *Phys. Chem. Chem. Phys.*, 13, 6484–6492, 2011.
- 651 Malloy, Q. G. J., Li Qi, Warren, B., Cocker III, D. R., Erupe, M. E., and Silva, P. J.:
652 Secondary organic aerosol formation from primary aliphatic amines with NO₃ radical, *Atmos.*
653 *Chem. Phys.*, 9, 2051–2060, 2009.
- 654 Martin, S. T., Artaxo, P., Machado, L. A. T., Manzi, A. O., Souza, R. A. F., Schumacher, C.,
655 Wang, J., Andreae, M. O., Barbosa, H. M. J., Fan, J., Fisch, G., Goldstein, A. H., Guenther,
656 A., Jimenez, J. L., Pöschl, U., Silva Dias, M. A., Smith, J. N., and Wendisch, M.: Introduction:
657 Observations and Modeling of the Green Ocean Amazon (GoAmazon2014/5), *Atmos.*
658 *Chem. Phys.*, 16, 4785–4797, 2016.
- 659 Martin, S. T., Andreae, M. O., Artaxo, P., Baumgardner, D., Chen, Q., Goldstein, A. H.,
660 Guenther, A., Heald, C. L., Mayol-Bracero, O. L., McMurry, P. H., Pauliquevis, T., Pöschl, U.,
661 Prather, K. A., Roberts, G. C., Saleska, S. R., Silva Dias, M. A., Spracklen, D. V., Swietlicki,
662 E., and Trebs, I.: Sources and properties of Amazonian aerosol particles, *Rev. Geophys.*, 48,
663 RG2002, doi:10.1029/2008RG000280, 2010.
- 664 Maryon, R.H., Smith, F.B., Conway, B.J., Goddard, D.M.: The U.K. nuclear accident model,
665 *Prog. Nucl. Energy* 26, 85–104, 1991.
- 666 Mazzoleni, L. R., Ehrmann, B. M., Shen, X., Marshall, A. G., and Collett Jr., J. L.: Water-
667 soluble atmospheric organic matter in fog: exact masses and chemical formula identification
668 by ultrahighresolution Fourier transform ion cyclotron resonance mass spectrometry,
669 *Environ. Sci. Technol.*, 44, 3690–3697, 2010.
- 670 Mazzoleni, L. R., Saranjampour, P., Dalbec, M. M., Samburova, V., Hallar, A. G., Zielinska,
671 B., Lowenthal, D., and Kohl, S.: Identification of water-soluble organic carbon in nonurban
672 aerosols using ultrahigh-resolution FT-ICR mass spectrometry: organic anions, *Environ.*
673 *Chem.*, 9, 285–297, 2012.
- 674 Müller, M., Mikoviny, T., Jud, W., D'Anna, B., and Wisthaler, A.: A New Software Tool for the
675 Analysis of High Resolution PTR-TOF Mass Spectra, *Chemometr. Intell. Lab.*, 127, 158–165,
676 2013.
- 677 Nguyen, Q. T., Christensen, M. K., Cozzi, F., Zare, A., Hansen, A. M. K., Kristensen, K.,
678 Tulinius, T. E., Madsen, H. H., Christensen, J. H., Brandt, J., Massling, A., Nøjgaard, J. K.,
679 and Glasius, M.: Understanding the anthropogenic influence on formation of biogenic



- 680 secondary organic aerosols in Denmark via analysis of organosulfates and related oxidation
681 products, *Atmos. Chem. Phys.*, 14, 8961–8981, 2014.
- 682 Nizkorodov, S. A., Laskin, J., and Laskin, A.: Molecular chemistry of organic aerosols
683 through the application of high resolution mass spectrometry, *Phys. Chem. Chem. Phys.*, 13,
684 3612–3629, 2011.
- 685 Nozière, B., Kalberer, M., Claeys, M., Allan, J., D’Anna, B., Decesari, S., Finessi, E.,
686 Glasius, M., Grgic, I., Hamilton, J. F., Hoffmann, T., Iinuma, Y., Jaoui, M., Kahnt, A., Kampf,
687 C. J., Kourtchev, I., Maenhaut, W., Marsden, N., Saarikoski, S., Schnelle-Kreis, J., Surratt,
688 J., Szidat, S., Szmigielski, R., and Wisthaler, S.: The molecular identification of organic
689 compounds in the atmosphere: state of the art and challenges, *Chem. Rev.*, 115, 3919–
690 3983, 2015.
- 691 Pashynska, V., Vermeylen, R., Vas, G., Maenhaut, W., and Claeys, M.: Development of a
692 gas chromatographic/ion trap mass spectrometric method for the determination of
693 levoglucosan and saccharidic compounds in atmospheric aerosols. Application to urban
694 aerosols. *J. Mass Spec.*, 37, 1249–1257, 2002.
- 695 Pöschl, U., Martin, S. T., Sinha, B., Chen, Q., Gunthe, S. S., Huffman, J. A., Borrmann, S.,
696 Farmer, D. K., Garland, R. M., Helas, G., Jimenez, J. L., King, S. M., Manzi, A., Mikhailov,
697 E., Pauliquevis, T., Petters, M. D., Prenni, A. J., Roldin, P., Rose, D., Schneider, J., Su, H.,
698 Zorn, S. R., Artaxo, P., and Andreae, M. O.: Rainforest aerosols as biogenic nuclei of clouds
699 and precipitation in the Amazon, *Science*, 429, 1513–1516, 2010.
- 700 Pye, H. O. T., Pinder, R. W., Piletic, I. R., Xie, Y., Capps, S. L., Lin, Y.-H., Surratt, J. D.,
701 Zhang, Z., Gold, A., Luecken, D. J., Hutzell, W. T., Jaoui, M., Offenberg, J. H., Kleindienst,
702 T. E., Lewandowski, M., and Edney, E. O.: Epoxide pathways improve model predictions of
703 isoprene markers and reveal key role of acidity in aerosol formation, *Environ. Sci. Technol.*,
704 47, 11056–11064, 2013.
- 705 Rasmussen, R.A. and Khalil, M.A.K.: Isoprene over the Amazon Basin. *J. Geophys. Res.*,
706 93: 1417–1427. doi: 10.1029/JD093iD02p01417JD093iD02p01417, 1988.
- 707 Reemtsma, T.: Determination of molecular formulas of natural organic matter molecules by
708 (ultra-) high-resolution mass spectrometry status and needs, *J. Chromatogr. A*, 1216, 3687–
709 3701, 2009.
- 710 Riva, M., Tomaz, S., Cui, T., Lin, Y.-H., Perraudin, E., Gold, A., Stone, E. A., Villenave, E.,
711 and Surratt, J. D.: Evidence for an unrecognized secondary anthropogenic source of
712 organosulfates and sulfonates: gas-phase oxidation of polycyclic aromatic hydrocarbons in
713 the presence of sulfate aerosol, *Environ. Sci. Technol.*, 49, 6654–6664, 2015.
- 714 Riva, M., Da Silva Barbosa, T., Lin, Y.-H., Stone, E. A., Gold, A., and Surratt, J. D.:
715 Characterization of Organosulfates in Secondary Organic Aerosol Derived from the
716 Photooxidation of Long-Chain Alkanes, *Atmos. Chem. Phys. Discuss.*, doi:10.5194/acp-
717 2016-20, 2016.
- 718 Ryall, D. B. and Maryon, R. H.: Validation of the UK Met Office’s NAME model against the
719 ETEX dataset, *Atmos. Environ.*, 32, 4265–4276, 1998.



- 720 Roberts, J. M.: The atmospheric chemistry of organic nitrates. *Atmos. Environ.*, 24,243-287,
721 1990.
- 722 Rincón, A. G., Calvo, A. I., Dietzel, M., and Kalberer, M.: Seasonal differences of urban
723 organic aerosol composition: an ultra-high resolution mass spectrometry study. *Environ.*
724 *Chem.*, 9, 298-319, 2012.
- 725 Schmitt-Kopplin, P., Gelencsér, A., Dabek-Zlotorzynska, E., Kiss, G., Hertkorn, N., Harir, M.,
726 Hong, Y., and Gebefügi, I.: Analysis of the unresolved organic fraction in atmospheric
727 aerosols with ultrahigh-resolution mass spectrometry and nuclear magnetic resonance
728 spectroscopy: Organosulfates as photochemical smog constituents, *Anal. Chem.*, 82, 8017–
729 8026, 2010.
- 730 Seco, R., Peñuelas, J., Filella, I., Llusia, J., Schallhart, S., Metzger, A., Müller, M., and
731 Hansel, A.: Volatile Organic Compounds in the Western Mediterranean Basin: urban and
732 rural winter measurements during the DAURE campaign, *Atmos. Chem. Phys.*, 13: 4291-
733 4306, 2013.
- 734 Simoneit, B. R. T., Schauer, J. J., Nolte, C. G., Oros, D. R., Elias, V. O., Fraser, M. P.,
735 Rogge, W. F. and Cass, G. R.: Levoglucosan, a tracer for cellulose in biomass burning and
736 atmospheric particles. *Atmos. Environ.*, 33, 173–182, 1999.
- 737 Surratt, J. D., Lewandowski, M., Offenberg, J. H., Jaoui, M., Kleindienst, T. E., Edney, E. O.,
738 and Seinfeld, J. H.: Effect of acidity on secondary organic aerosol formation from isoprene,
739 *Environ. Sci. Technol.*, 41, 5363–5369, 2007.
- 740 Surratt, J. D., Gomez-Gonzalez, Y., Chan, A. W. H., Vermeylen, R., Shahgholi, M.,
741 Kleindienst, T. E., Edney, E. O., Offenberg, J. H., Lewandowski, M., Jaoui, M., Maenhaut,
742 W., Claeys, M., Flagan, R. C., and Seinfeld, J. H.: Organosulfate formation in biogenic
743 secondary organic aerosol, *J. Phys. Chem. A*, 112, 8345–8378, 2008.
- 744 Surratt, J. D., Chan, A. W. H., Eddingsaas, N. C., Chan, M. N., Loza, C. L., Kwan, A. J.,
745 Hersey, S. P., Flagan, R. C., Wennberg, P. O., and Seinfeld, J. H.: Reactive intermediates
746 revealed in secondary organic aerosol formation from isoprene, *P. Natl. Acad. Sci. USA*,
747 107, 6640–6645, 2010.
- 748 Song, C., Gyawali, M., Zaveri, R. A., Shilling, J. E., and Arnott, W. P.: Light absorption by
749 secondary organic aerosol from α -pinene: Effects of oxidants, seed aerosol acidity, and
750 relative humidity, *J. Geophys. Res.*, 118 (20), 11741-11749, doi: 10.1002/jgrd.50767, 2013.
- 751 Szmigielski, R., Surratt, J. D., Gomez-Gonzalez, Y., Van der Veken, P., Kourtchev, I.,
752 Vermeylen, R., Blockhuys, F., Jaoui, M., Kleindienst, T. E., Lewandowski, M., Offenberg, J.
753 H., Edney, E. O., Seinfeld, J. H., Maenhaut, W., and Claeys, M.: 3-methyl-1,2,3-
754 butanetricarboxylic acid: An atmospheric tracer for terpene secondary organic aerosol,
755 *Geophys. Res. Lett.*, 34, L24811, doi:10.1029/2007GL031338, 2007.
- 756 Tao, S., Lu, X., Levac, N., Bateman, A. P., Nguyen, T. B., Bones, D. L., Nizkorodov, S. A.,
757 Laskin, J., Laskin, A., and Yang, X.: Molecular characterization of organosulfates in organic
758 aerosols from Shanghai and Los Angeles urban areas by nanospray-desorption electrospray
759 ionization high-resolution mass spectrometry, *Environ. Sci. Technol.*, 48, 10993–11001,
760 2014.



- 761 Tong, H., Kourtchev, I., Pant, P., Keyte, I., O'Connor, I., Wenger, J., Pope, F.D., Harrison,
762 R.M., and Kalberer, M.: FDATA16 Molecular Composition of Organic Aerosols at Urban
763 Background and Road Tunnel sites using Ultra-high Resolution Mass Spectrometry, Faraday
764 Discuss., DOI: 10.1039/C5FD00206K, 2016.
- 765 Wang, X.K., Rossignol, S., Ma, Y., Yao, L., Wang, M.Y., Chen, J.M., George, C., and Wang,
766 L.: Identification of particulate organosulfates in three megacities at the middle and lower
767 reaches of the Yangtze River, Atmos. Chem. Phys. Discuss., 15, 21414-21448, 2015.
- 768 Wozniak, A. S., Bauer, J. E., Sleighter, R. L., Dickhut, R. M., and Hatcher, P. G.: Technical
769 Note: Molecular characterization of aerosol-derived water soluble organic carbon using
770 ultrahigh resolution electrospray ionization Fourier transform ion cyclotron resonance mass
771 spectrometry, Atmos. Chem. Phys., 8, 5099– 5111, 2008.
- 772 Yassine, M. M., Harir, M., Dabek-Zlotorzynska, E., and Schmitt-Kopplin, P: Structural
773 characterization of organic aerosol using Fourier transform ion cyclotron resonance mass
774 spectrometry: aromaticity equivalent approach. Rapid Commun. Mass Sp., 28, 2445-2454,
775 2014.
- 776 Zahardis, J., Geddes, S., and Petrucci, G. A.: The ozonolysis of primary aliphatic amines in
777 fine particles, Atmos. Chem. Phys., 8, 1181-1194, 2008.
- 778 Zhao, Y., Hallar, A. G., and Mazzoleni, L. R.: Atmospheric organic matter in clouds: exact
779 masses and molecular formula identification using ultrahigh-resolution FT-ICR mass
780 spectrometry, Atmos. Chem. Phys., 13, 12343-12362, 2013.

781

782

783

784

785

786

787

788

789

790

791

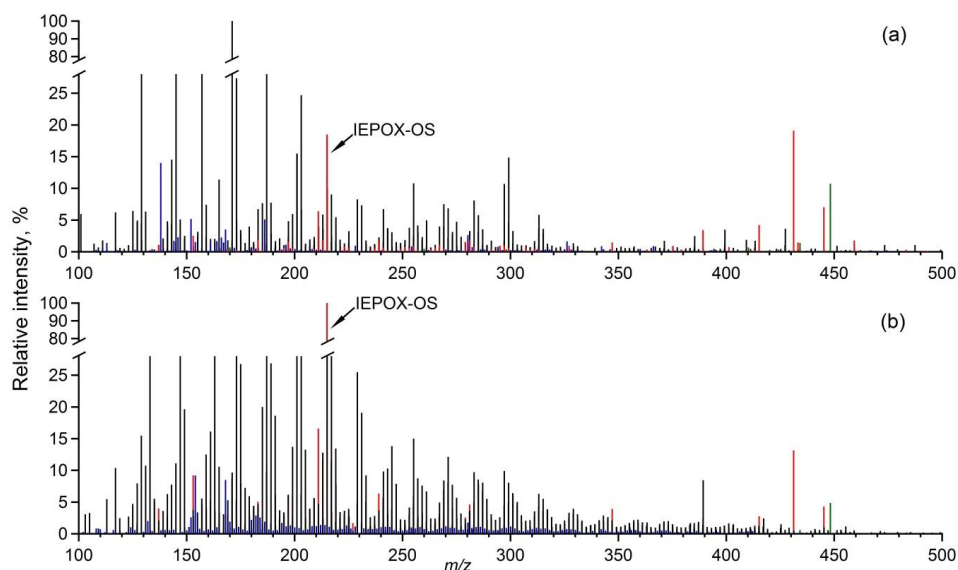
792

793

794

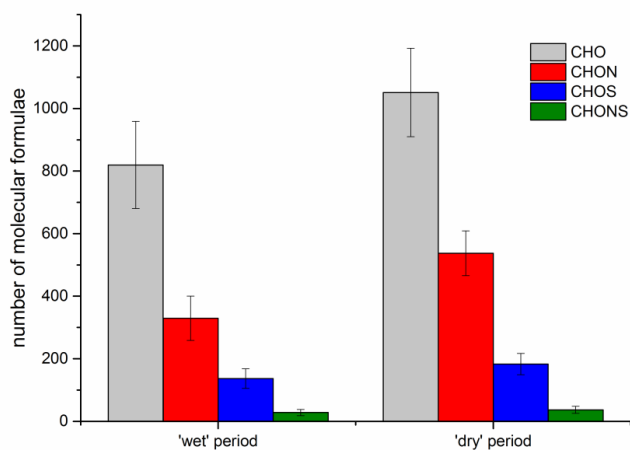


795 **Figures:**



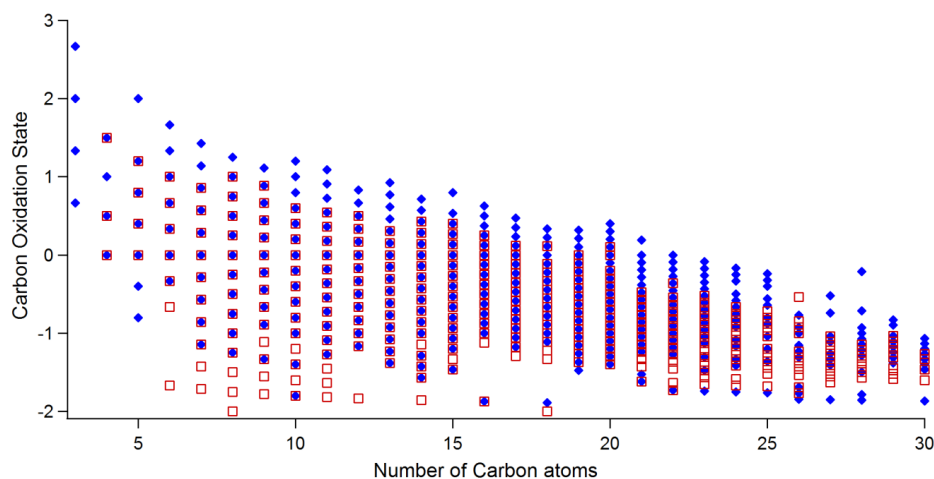
796

797 Figure 1. (-)-nanoESI-UHRMS of the representative PM2.5 samples during (a) IOP1 (b)
 798 IOP2. The line colours in the mass spectra correspond to the CHO (black), blue (CHON),
 799 CHOS (red) and CHONS (green) formulae assignments. The relative intensity axis was split
 800 to make a large number of ions with low intensities visible.



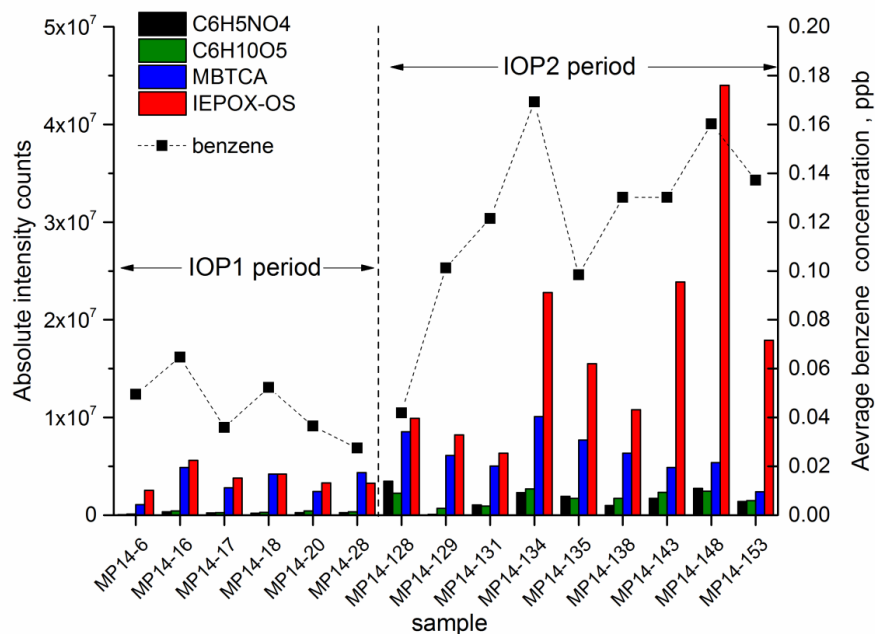
801

802 Figure 2. Average number of molecular formulae during IOP1 and IOP2. Standard deviation
 803 bars show variations between samples within individual season.



804

805 Figure 3. Carbon oxidation state plot for CHO containing formulae in organic aerosol from
 806 IOP1 (red squares) and IOP2 (blue diamonds).

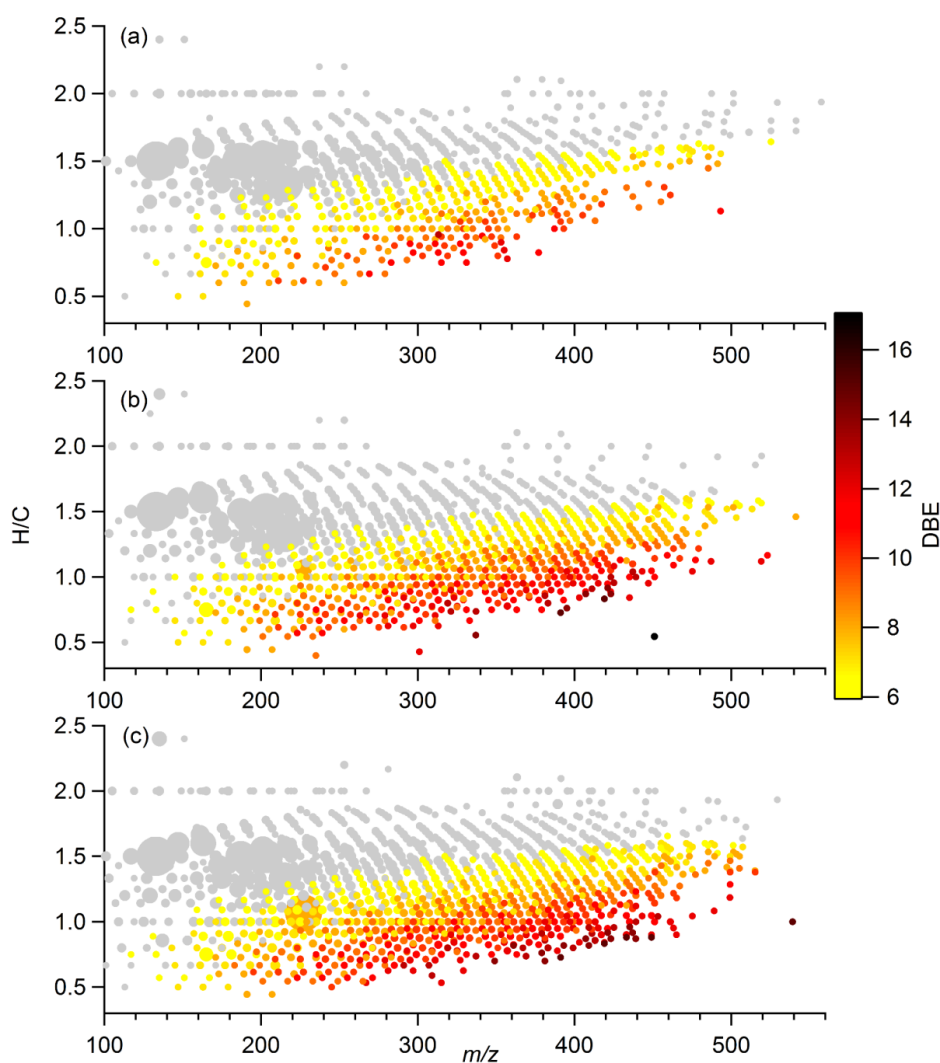


807

808 Figure 4. Ion intensity distributions (left axis) of selected tentatively identified markers in
 809 individual samples using UHRMS analysis and averaged benzene concentration (right axis)
 810 from PTR-TOF-MS analysis. Benzene concentration was averaged for the aerosol filter
 811 sampling intervals. The UHRMS data was corrected for organic carbon load in each
 812 individual filter sample (see method section).



813

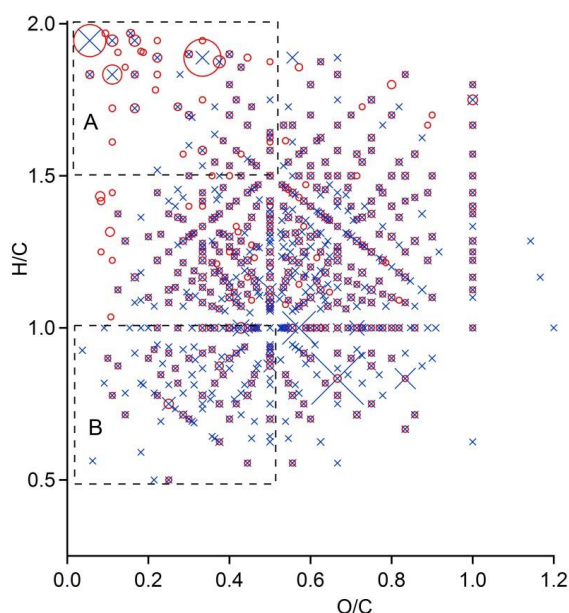


814

815 Figure 5. H/C vs m/z plot for CHO containing formulae in the samples from the periods with
 816 (a) low (b) moderately high and (c) very high incidents of fires. The marker areas reflect
 817 relative ion abundance in the sample. The colour code shows double bond equivalent (DBE)
 818 in the individual molecular formula. Molecular formulae with DBE<6 are shown as grey
 819 markers.

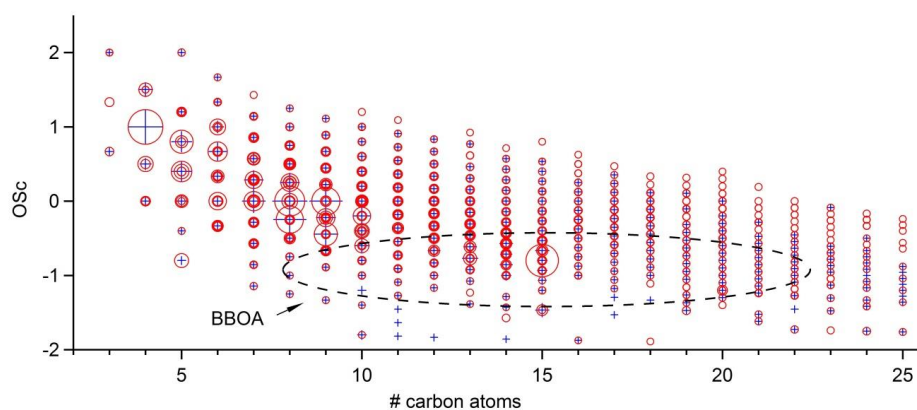
820

821



822

823 Figure 6. Overlaid Van Krevelen diagrams for CHON containing formulae in the samples
 824 from the periods with low (red markers) and very high incidents (blue markers) of fires. The
 825 marker areas reflect relative ion abundance in the sample. Areas 'A' and 'B' indicate
 826 differences in the number of ions tentatively attributed to aliphatic and aromatic species,
 827 respectively.



828

829 Figure 7. Overlaid carbon oxidation state (OSc) plots for CHO subgroups in the samples
 830 from the periods with low (blue markers) and very high (red markers) incidents of fires. The
 831 marker areas reflect relative ion abundance in the sample. The area marked as BBOA
 832 correspond to the molecules associated with biomass burning organic aerosol as outlined by
 833 Kroll et al. (2011).

834

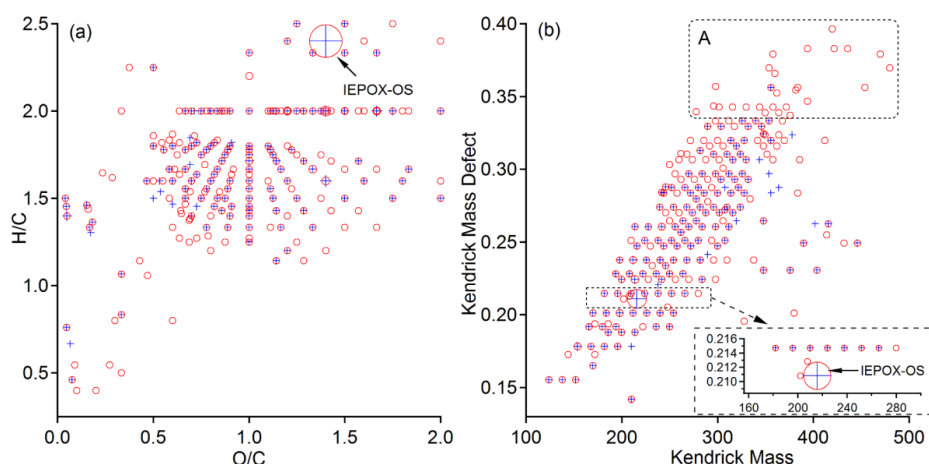


Figure 8. Overlaid Van Krevelen diagram (a) and Kendrick Mass Defect plot (b) for CHOS containing formulae in the samples from the periods with low (blue markers) and very high incidents of fires (red markers). The marker areas reflect relative ion abundance in the sample. Red markers correspond to the ions from the period with the lowest incidents of fires. Note that IEPOX-OS is not a part of any homologous series in the sample with very low incident of fires and only one additional homologue in the sample that experienced very high incident of fires (see enlarged area of the Fig 8a). Area 'A' in Kendrick Mass Defect (KMD) plot shows formulae with KMD>0.33 that are mainly present in the sample with high incident of fires.